



# Rapid Pacing Decreases L-type $\text{Ca}^{2+}$ Current and Alters *Cacna1c* Isoform Expression in Primary Cultured Rat Left Ventricular Myocytes

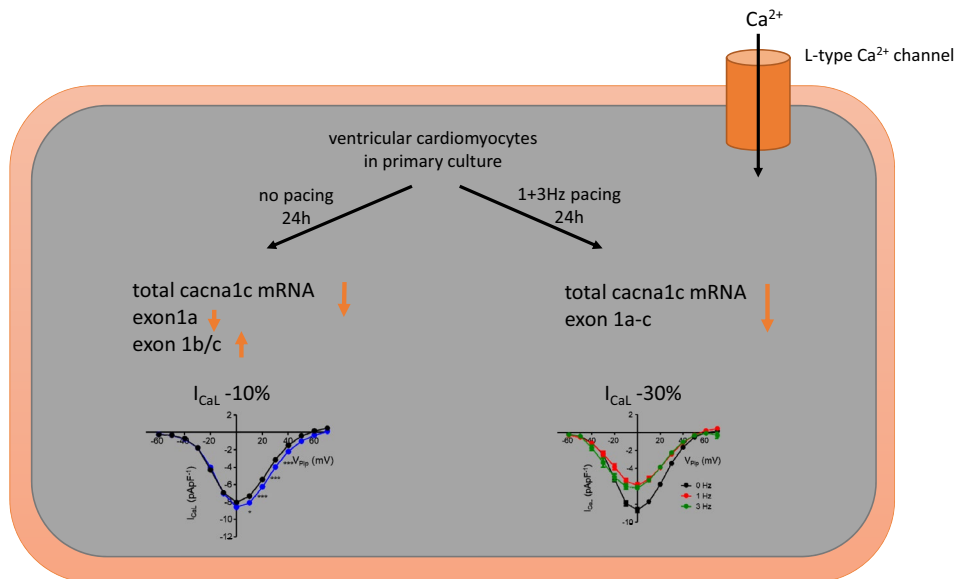
Anne Ritzer<sup>1</sup> · Tobias Roeschl<sup>1</sup> · Sandra Nay<sup>1</sup> · Elena Rudakova<sup>1</sup> · Tilmann Volk<sup>1,2</sup>

Received: 5 September 2022 / Accepted: 14 March 2023 / Published online: 30 March 2023  
© The Author(s) 2023

## Abstract

The L-type calcium current ( $I_{\text{CaL}}$ ) is the first step in cardiac excitation–contraction-coupling and plays an important role in regulating contractility, but also in electrical and mechanical remodeling. Primary culture of cardiomyocytes, a widely used tool in cardiac ion channel research, is associated with substantial morphological, functional and electrical changes some of which may be prevented by electrical pacing. We therefore investigated  $I_{\text{CaL}}$  directly after cell isolation and after 24 h of primary culture with and without regular pacing at 1 and 3 Hz in rat left ventricular myocytes. Moreover, we analyzed total mRNA expression of the pore forming subunit of the L-type  $\text{Ca}^{2+}$  channel (*cacna1c*) as well as the expression of splice variants of its exon 1 that contribute to specificity of  $I_{\text{CaL}}$  in different tissue such as cardiac myocytes or smooth muscle. 24 h incubation without pacing decreased  $I_{\text{CaL}}$  density by ~ 10% only. Consistent with this decrease we observed a decrease in the expression of total *cacna1c* and of exon 1a, the dominant variant of cardiomyocytes, while expression of exon 1b and 1c increased. Pacing for 24 h at 1 and 3 Hz led to a substantial decrease in  $I_{\text{CaL}}$  density by 30%, mildly slowed  $I_{\text{CaL}}$  inactivation and shifted steady-state inactivation to more negative potentials. Total *cacna1c* mRNA expression was substantially decreased by pacing, as was the expression of exon 1b and 1c. Taken together, electrical silence introduces fewer alterations in  $I_{\text{CaL}}$  density and *cacna1c* mRNA expression than pacing for 24 h and should therefore be the preferred approach for primary culture of cardiomyocytes.

## Graphical Abstract



Anne Ritzer and Tobias Roeschl have contributed equally to this work.

Extended author information available on the last page of the article

**Keywords** *Cacna1c* · Cardiac memory · Regional differences · Remodeling

## Introduction

### Function of L-type Calcium Channel in the Heart and Alternative Splicing

The L-type  $\text{Ca}^{2+}$  current ( $I_{\text{CaL}}$ ) contributes to shape and duration of the ventricular action potential (AP) in the heart of many species including rodents, canine and man (Cora-boeuf and Nargeot 1993; Linz and Meyer 2000). Moreover,  $\text{Ca}^{2+}$  influx via the L-type  $\text{Ca}^{2+}$  channel is the first step in the excitation–contraction-coupling cascade, its magnitude controls the amount of  $\text{Ca}^{2+}$  released from the sarcoplasmic reticulum (SR) and contributes to the filling status of the SR thereby contributing to the control of contractile force (Eisner et al. 2017; Gambardella et al. 2018). Accordingly, acute changes in the magnitude of  $I_{\text{CaL}}$  in- or decrease cardiac contractility and hence, cardiac output. The intracellular  $\text{Ca}^{2+}$  concentration not only controls contractility, but is also a potent regulator of gene expression (Dewenter et al. 2017). Long term changes in  $I_{\text{CaL}}$  magnitude are therefore considered an early step in the development of cardiac pathologies such as hypertrophy or heart failure and contribute to electrical and structural remodeling (Muth et al. 2001; Bosch et al. 2003; Chen-Izu et al. 2007; Zhang et al. 2016).

In addition to cardiac myocytes, L-type  $\text{Ca}^{2+}$  channels are widely expressed in various excitable and non-excitable tissues such as striated and smooth muscle, neurons, endocrine glands or fibroblasts, where they serve different and specific functions such as control of excitability, hormonal release or gene expression (Moosmang et al. 2003; Marcantoni et al. 2007; Calin-Jageman and Lee 2008; Zamponi et al. 2015). Tissue specific function of L-type  $\text{Ca}^{2+}$  channels originates to some extent from specific expression of four different variants of the pore-forming  $\alpha$ -subunit ( $\text{Ca}_v1.1$ – $1.4$ ) (Feng et al. 2018). Moreover, the  $\alpha$ -subunits associate with additional  $\beta$ - and  $\delta$ -subunits that modify expression levels and functional characteristics (Tseng et al. 2006). Of the four variants,  $\text{Ca}_v1.1$  is mainly found in skeletal muscle and is crucial for contraction (Wu et al. 2017) whereas  $\text{Ca}_v1.2$  and  $1.3$  show somewhat overlapping expression patterns and are located in adrenal chromaffin cells (Vandael et al. 2013), cardiac tissue (Bodi et al. 2005; Feng et al. 2018) and neuronal cells (Berger and Bartsch 2014). Furthermore,  $\text{Ca}_v1.3$  is also found in the pancreas and the kidney and is essential for endocrine secretion (Barnett et al. 1995; Nitert et al. 2008) as well as in the cochlea contributing to auditory transduction (Brandt et al. 2003; Michna et al. 2003).  $\text{Ca}_v1.4$  is mainly expressed in retinal cells and necessary for normal

visual function (Lee et al. 2015). The cardiac variant of the  $\alpha$ -subunit,  $\text{Ca}_v1.2$ , is also expressed in smooth muscle and in neurons. Functional specificity of L-type  $\text{Ca}^{2+}$  channels not only originates from the different pore-forming  $\alpha$ -subunits, but also from alternative splicing of the same  $\alpha$ -subunit. In fact, in humans, the gene encoding  $\text{Ca}_v1.2$ , *cacna1c*, is composed of at least 55 exons of which 19 undergo alternative splicing (Abernethy and Soldatov 2002; Tang et al. 2004). The corresponding gene in rats contains 52 exons with alternative splicing occurring in at least 11 of them (Tang et al. 2004; Wang et al. 2006). A number of studies have conferred functional differences of  $I_{\text{CaL}}$  in different tissues to alternative splicing. For example, activation and inactivation potentials of  $I_{\text{CaL}}$  in smooth muscle cells are shifted to more positive potentials presumably by expression of different splice variants of exons 1, 8 and 33 (Biel et al. 1991; Liao et al. 2005; Lipscombe & Andrade 2015). However, there is a large overlap in splice variant expression in different tissues. Exon 1a is exclusively expressed in cardiac myocytes whereas exon 1b is also found in smooth muscle cells and neurons (Snutch et al. 1991; Hofmann et al. 2014). A third variant of exon 1, exon 1c is also expressed in both cardiomyocytes and smooth muscle cells of resistance size cerebral arteries and is of particular importance for the smooth muscle phenotype of  $I_{\text{CaL}}$  (Cheng et al. 2007). It is therefore not surprising, that exon 1a-c expression quantitatively differs substantially between cardiac and smooth muscle cells. In cardiac myocytes, exon 1a accounts for ~80% of total exon 1 mRNA, exon 1b for ~5% and exon 1c for 15%. In contrast, in smooth muscle cells exon 1a is not expressed, exon 1b accounts for ~5% and exon 1c for 95% (Cheng et al. 2007).

Primary culture of isolated adult ventricular myocytes is a common and widely used tool to investigate non-acute effects (in the range of days) of drugs or hormones, signaling cascades or even altered gene expression on cardiomyocyte morphology or function. However, deprived of their natural environment primary cultured ventricular myocytes undergo substantial morphological and functional changes. They lose their rectangular shape, decrease in cell surface area, undergo alterations in the t-tubular system and the amplitude of their  $\text{Ca}^{2+}$  transient decreases as well as their contractility (Banyasz et al. 2008; Parameswaran et al. 2013; Seidel et al. 2019; Kim et al. 2020). With respect to  $I_{\text{CaL}}$ , its amplitude has been found to decrease over days with slower inactivation and increased half-decay time of the  $\text{Ca}^{2+}$  transient (Banyasz et al. 2008; Kim et al. 2020). Regular pacing has been suggested to mitigate some negative effects of primary culture as it maintained contractility of isolated cardiac

myocytes in primary culture (Berger et al. 1994). Moreover, regular pacing contributes to the stability of isolated ventricular tissue in culture (Fischer et al. 2019) and improves the differentiation of stem cells into ventricular cardiomyocytes (Nunes et al. 2013; Hirt et al. 2014; Ruan et al. 2016).

In the present study we investigated the effect of 24 h primary culture with and without pacing at 1 or 3 Hz on amplitude and kinetics of  $I_{\text{CaL}}$ . We assessed total *cacna1c* mRNA expression and analyzed the expression of the three different variants of exon 1 to determine whether primary culture with or without pacing leads to alterations in isoform expression of the L-type  $\text{Ca}^{2+}$  channel  $\alpha$ -subunit. We show that 24 h primary culture leads to a small but significant decrease in  $I_{\text{CaL}}$ , but a substantially decrease in *cacna1c* total mRNA expression and in the expression of the cardiac isoform of exon 1 while exon 1b and exon 1c expression increased. Pacing with 1 or 3 Hz substantially decreased  $I_{\text{CaL}}$  amplitude and *cacna1c* total mRNA expression as well as the cardiac isoform of exon 1, whereas exon 1b and exon 1c expression remained unaltered.

## Methods

### Isolation of Myocytes

Cardiomyocytes were isolated from the left ventricular free wall of female Wistar rats (~220 g) as described previously (Wagner et al. 2010; Wacker et al. 2020). After induction of deep anesthesia by intraperitoneal injection of thiopental-sodium (100 mg  $\text{kg}^{-1}$  body mass), the heart was quickly excised and placed into cold (4 °C) Tyrode's solution. Subsequently, the aorta was retrogradely perfused for 5 min with modified Tyrode's solution containing 4.5 mM  $\text{Ca}^{2+}$  and 5 mM EGTA (~1  $\mu\text{M}$  free  $\text{Ca}^{2+}$  concentration). The perfusion was continued for 19 min, recirculating 25 ml of the same solution containing collagenase (CLS type II, 160 U/ml, Biochrom KG, Berlin, Germany) and protease (type XIV, 0.6 U/ml, Sigma). Then, the heart was perfused for another 5 min with storage solution containing 100  $\mu\text{M}$   $\text{Ca}^{2+}$ . The left ventricular free wall was separated from the rest of the heart and dissected into small tissue pieces. Tissue pieces were further minced and gently agitated to obtain single cardiomyocytes. Myocytes were stepwise adapted to physiological  $\text{Ca}^{2+}$  levels, transferred to six-well cell culture dishes containing M199 medium (Sigma) supplemented with 1 mg/mL bovine serum albumin (BSA, Roth) and penicillin/streptomycin (Biochrom) and stored at 37 °C in a water-saturated atmosphere containing 5%  $\text{CO}_2$ . After a period of three hours, carbon-based pacing electrodes (C-Dish, IonOptix) were introduced into the six-well cultures dishes and 24 h pacing was initiated at 1 or 3 Hz using a bi-phasic stimulus of 7 ms duration. The pacing voltage

stimulus was set to a level that ~90% of the myocytes contracted and ranged from 10.5 V to 14.5 V.

All experiments were performed in accordance with relevant guidelines and regulations and all experimental protocols were approved by the Regierung von Mittelfranken, license No: 621-2531.32-11/05.

### Patch-Clamp Technique

The ruptured-patch whole-cell configuration was used as described previously (Wagner et al. 2008). Myocardial cells were transferred into an elongated chamber (4×20 mm), mounted on the stage of an inverted microscope (Axiovert 40, Zeiss, Jena, Germany) and initially superfused with control solution. All experiments were performed at room temperature (22–25 °C). Patch pipettes were pulled from borosilicate glass (GC150-15, Clark Electromedical Instruments, Reading, UK) using a P-97 Puller (Sutter Instruments, Novato, CA, USA). Pipette resistance ( $R_{\text{pip}}$ ) was 1.5–5 M $\Omega$ . Currents were recorded using an EPC-10 amplifier (HEKA Elektronik, Lambrecht, Germany), controlled by PULSE-Software (HEKA Elektronik). Membrane capacitance ( $C_m$ ) and series resistance ( $R_s$ ) were calculated using the automated capacitance compensation procedure of the EPC-10 amplifier. Series resistance was in the range of ~5 M $\Omega$ , was not allowed to exceed 10 M $\Omega$  and was compensated by 85%. The reference electrode of the amplifier headstage was bathed in pipette solution in a separate chamber and was connected to the bath solution via an agar–agar bridge filled with pipette solution. Pipette potentials ( $V_{\text{pip}}$ ) were corrected for liquid junction potentials at the bridge–bath junction. Whole-cell currents were low-pass filtered at 1 kHz and sampled at 5 kHz.

To assess  $I_{\text{CaL}}$ , myocytes were clamped for 600 ms from the holding potential of –90 mV to test potentials between –60 mV and +70 mV in steps of 10 mV.  $\text{Na}^+$  currents were inactivated by a prepulse of 70 ms to –50 mV. In some experiments, if a residual  $\text{Na}^+$  current was still present, the prepulse voltage was decreased to  $V_{\text{pip}} = -45$  mV. Basic cycle length was 3000 ms.  $I_{\text{CaL}}$  was quantified by subtracting the current at the end of the test pulse from the peak current. To determine activation kinetics, the slope conductance ( $G_{\text{CaL}}$ ) of  $I_{\text{CaL}}$  was calculated for each pipette potential ( $G_{\text{CaL}} = I_{\text{CaL}} / (V_{\text{pip}} - V_{\text{rev}})$ ) where  $V_{\text{rev}}$  is the apparent reversal potential of  $I_{\text{CaL}}$ .  $G_{\text{CaL}}$  was then normalized to the maximal observed slope conductance recorded in each individual experiment and plotted vs. the pipette potential. Steady-state inactivation was determined by a two-step pulse protocol: a conditioning pulse of 600 ms duration from  $V_{\text{pip}} = -90$  mV to +10 mV in steps of 10 mV was followed by a test pulse to  $V_{\text{pip}} = 0$  mV for 600 ms. The magnitude of  $I_{\text{CaL}}$  of each test pulse was normalized to  $I_{\text{CaL}}$  recorded at a conditioning potential of  $V_{\text{pip}} = -80$  mV in each individual experiment and plotted vs. the pulse potential. Activation and steady-state inactivation were fitted using the Boltzmann equation.

Recovery from inactivation was determined by two consecutive pulses to  $V_{\text{pip}} = 0$  mV of 600 ms duration, separated by a repolarization to  $V_{\text{pip}} = -90$  mV. The duration of the interval ranged from 5 to 1500 ms and increased by a factor 1.5 from step to step. The holding potential was  $V_{\text{pip}} = -90$  mV, cycle length was 5000 ms. The magnitude of  $I_{\text{CaL}}$  recorded during the second voltage pulse was normalized to the magnitude of the first, plotted vs. the duration of the interval between the voltage pulses and the resulting curve was fitted using a mono-exponential equation.

### Quantitative Real Time PCR Analysis

Fresh or paced rat cardiomyocytes were centrifuged for 5 min at 1000 g and the pellets were immediately frozen at  $-80$  °C. RNA-isolation was performed using the NucleoSpin RNA-Kit from Macherey–Nagel, applying the manufacturer's protocol for cells and tissue. RNA-concentration of each sample was measured with the Denovix DS 11 + spectrophotometer. Using the QuantiTect reverse transcription kit from Qiagen, single-stranded cDNA was synthesized from 50 µg total RNA. Quantitative real time PCR was performed in the StepOnePlus cycler from Applied Biosystems, using the following sequence: 2 min at 50 °C and 2 min at 95 °C, then 40 cycles of 15 s at 95 °C and 1 min 60 °C and for the melt curve stage 15 s 95 °C, 1 min 60 °C and in 0.3 °C steps to 95 °C for 15 s. Analysis was performed using the Step One software, Microsoft Excel (Microsoft Corporation, Redmond, USA) and Prism (GraphPad, San Diego, USA). Specificity of primers was verified by PCR and gel electrophoresis followed by DNA sequencing. Samples were loaded in duplicates. The amplification efficiency for each gene was determined by a four-step serial dilution (five-fold) of the template. After correction for amplification efficiency, PCR results were normalized the arithmetic mean expression level of the three housekeeping genes (Gapdh, Hprt1 and Eef2). Fold change was calculated as a ratio of treated over control.

### Solutions and Primers

For the isolation of myocytes, modified Tyrode's solution contained (in mM): NaCl 138, KCl 4, Glucose 10,  $\text{NaH}_2\text{PO}_4$  0.33,  $\text{MgCl}_2$  1, HEPES 10,  $\text{CaCl}_2$  0.9, EGTA 1, Insulin  $10^{-3}$ , titrated to pH 7.30 using NaOH. The same solution with 2 mM  $\text{Ca}^{2+}$  was used as bath solution for the patch-clamp and fluorescence imaging experiments. For cell digestion, collagenase (162.8 U/ml, CLSII, Biochrom AG, Berlin, Deutschland) and protease (0.54 U/ml, type XIV, Sigma-Aldrich GmbH, Steinheim, Deutschland) were added to modified Tyrode's solution ( $10^{-6}$  M  $\text{Ca}^{2+}$ ). Storage solution contained (in mM): NaCl 130,  $\text{NaH}_2\text{PO}_4$  0.4,  $\text{NaHCO}_3$  5.8,  $\text{MgCl}_2$  0.5,  $\text{CaCl}_2$  1, KCl 5.4, glucose 22, and HEPES 25,

titrated to pH 7.40 with NaOH in the presence of 5%  $\text{CO}_2$  and supplemented with 1 mg  $\text{ml}^{-1}$  BSA. For recording  $\text{Ca}^{2+}$  currents, the pipette solution contained (in mM): CsCl 130,  $\text{MgCl}_2$  5, EGTA 10, HEPES 10,  $\text{Na}_2\text{ATP}$  2, pH 7.20 with CsOH. The concentration of free ionized  $\text{Ca}^{2+}$  in this solution was calculated using the approach published by Schoenmakers et al. (Schoenmakers et al. 1992) and was  $\sim 0.4$  nM ( $\text{pCa} \sim 9.4$ ).

Gene	Primer 5'- 3'
Exon 5	fw: gagagctttccgtgtgcttc rev: ccttgatgatggagttcagga
Exon 1a	fw: aaggtgtgtacacgaagctcaa rev: cgtgggctcccatagttg
Exon 1b	fw: caatggcaatgaaaacacga rev: ggctcccatagttggaacct
Exon 1c	fw: ctaggaagtgcagtaatgacctg rev: gttggaacatgcacagctccagag
Gapdh	fw: tgggaagctggtcatcaac rev: gcatcacccttctgatgtt
Hprt1	fw: cccagcgtcgtgattagtgga rev: tcgagcaagctttcagctct
Eef2	fw: aggccccatgggtattaaga rev: aaggcatagaagcggccttt

### Data Analysis and Statistics

Patch Clamp data were analyzed using the PULSE-FIT software (HEKA Elektronik, Lambrecht/Pfalz, Germany), IGOR Pro (WaveMetrics, Lake Oswego, USA), and Microsoft Excel as described previously (Foltz et al. 2012). Data are given as mean  $\pm$  SEM. Statistical significance was evaluated by unpaired Student's t test when two groups were compared or one-way ANOVA followed by Newman-Keuls test when more than two groups were compared using Prism.  $p < 0.05$  was considered statistically significant.

## Results

### Primary Culture and Pacing with 1 and 3 Hz Decreases L-type $\text{Ca}^{2+}$ Current Amplitude

It has been reported that L-type  $\text{Ca}^{2+}$  current ( $I_{\text{CaL}}$ ) of freshly isolated rat left ventricular myocytes decreases (Banyasz et al. 2008), remains stable (Yang et al. 2012) or increases (Ellingsen et al. 1993) during 24 h of primary culture. We therefore first investigated  $I_{\text{CaL}}$  amplitude directly after cell isolation (0–8 h) and after 24 h (24–32 h) of primary culture to investigate if and to what extent 24 h primary culture affects  $I_{\text{CaL}}$  amplitude and kinetics under our experimental conditions. Figure 1A displays representative current traces obtained from a myocyte directly after isolation (blue) and



after 24 h incubation (black).  $I_{\text{CaL}}$  traces appear quite similar. Figure 1B summarizes similar experiments and shows average current–voltage ( $I$ – $V$ ) relations, recorded from myocytes directly after isolation (blue) and after 24 h incubation (black). On average  $I_{\text{CaL}}$  decreased to a small ( $\sim 10\%$ ) but significant extent at command potentials from  $V_{\text{Pip}} = 10$  to 40 mV. Peak  $I_{\text{CaL}}$  recorded at  $V_{\text{Pip}} = 0$  mV decreased from  $-9.2 \pm 0.3$  pApF $^{-1}$  ( $n = 67$ ) to  $-8.3 \pm 0.3$  pApF $^{-1}$  ( $n = 62$ ,  $p = 0.057$ ). To address inactivation of  $I_{\text{CaL}}$  a biexponential function was fitted to the current decay at  $V_{\text{Pip}} = 0$  mV, hence yielding two time constants of inactivation,  $\tau_1$  and  $\tau_2$  (Wagner et al. 2008). Table 1 summarizes  $I_{\text{CaL}}$  inactivation. Neither  $\tau_1$  or  $\tau_2$ , nor their relative contribution to total inactivation was affected by 24 h incubation of the myocytes. Figure 1C shows average steady-state activation and steady-state

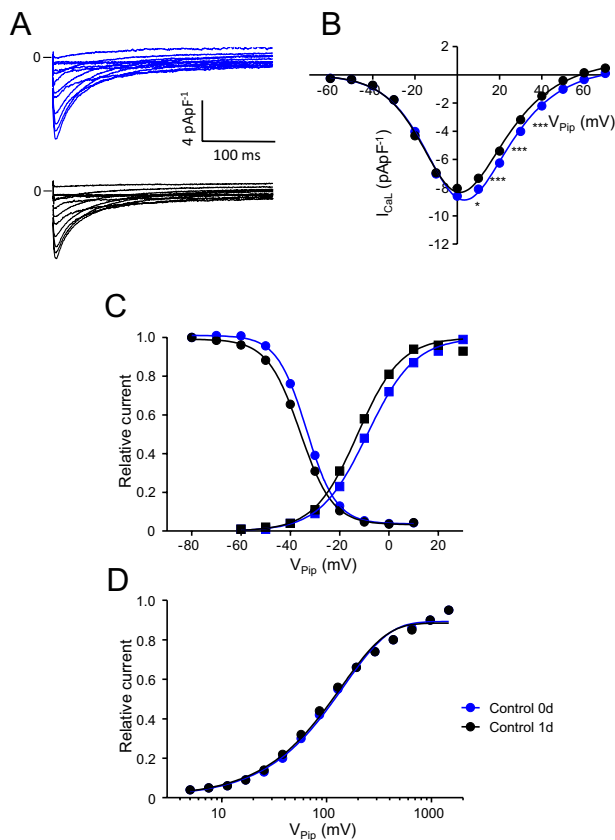


**Fig. 1** Primary culture (24–32 h) decreases  $I_{\text{CaL}}$  density. **A** representative whole-cell current traces of  $I_{\text{CaL}}$  recorded from freshly isolated myocytes (blue traces, ‘Control 0d’) and myocytes incubated for 24–32 h without pacing (black traces, ‘Control 1d’). **B** average current–voltage relations of currents similar to those shown in (A).  $I_{\text{CaL}}$  was quantified by subtracting the peak current from the current at the end of the voltage pulse (at 600 ms). **C** activation (circles) and steady-state inactivation (boxes) of  $I_{\text{CaL}}$  recorded from both groups. **D** recovery from inactivation of  $I_{\text{CaL}}$  recorded from both groups. For details regarding pulse protocols see methods section. Note that error bars are smaller than the symbols.  $56 \leq n \leq 111$ . \* $p < 0.05$ , \*\*\* $p < 0.001$ , Control 0d vs. Control 1d

**Table 1** Inactivation time constant of  $I_{\text{CaL}}$  after 24–32 h primary culture

	n	$\tau_1$ (ms)	$\tau_2$ (ms)	% $\tau_1$ (%)	% $\tau_2$ (%)
Control 0d	66	$20.1 \pm 0.7$	$105 \pm 2.9$	$67.4 \pm 0.7$	$32.6 \pm 0.7$
Control 1d	60	$20.2 \pm 0.7$	$108 \pm 3.0$	$67.0 \pm 0.7$	$33.0 \pm 0.7$

$\tau_1$  and  $\tau_2$  inactivation time constants of  $I_{\text{CaL}}$  obtained by bi-exponentially fitting of current decay at  $V_{\text{Pip}} = 0$  mV, %  $\tau_1$  and %  $\tau_2$  contribution of  $\tau_1$  and  $\tau_2$  to total inactivation (values are given in % of total inactivation),  $n$  number of myocytes

inactivation curves obtained from myocytes directly after isolation (blue) and after 24 h incubation (black). 24 h incubation significantly shifted steady-state activation and inactivation to more negative potentials from  $-8.6 \pm 0.5$  mV ( $n = 68$ ) to  $-12.8 \pm 0.6$  mV ( $n = 62$ ,  $p < 0.001$ ) and from  $-33.4 \pm 0.4$  mV ( $n = 111$ ) to  $-36.4 \pm 0.5$  mV ( $n = 72$ ,  $p < 0.001$ ), respectively and led to a small increase in the slope factor of steady-state inactivation from  $-5.4 \pm 0.1$  mV ( $n = 111$ ) to  $-6.2 \pm 0.1$  mV ( $n = 72$ ,  $p < 0.001$ ) (detailed parameters are summarized in Table 2). Recovery from inactivation (Fig. 1D) was not significantly affected by 24 h incubation and followed a monoexponential characteristic with an average time constant of  $154.1 \pm 4.8$  ms ( $n = 77$ ) in freshly isolated myocytes and  $148.9 \pm 7.1$  ms ( $n = 56$ , n.s.) in myocytes after 24 h incubation.

Next, we investigated, whether continuous pacing over 24 h at a low rate of 1 Hz or at a higher rate of 3 Hz prevented the observed decrease in  $I_{\text{CaL}}$ . Figure 2 shows representative current traces obtained from left ventricular myocytes incubated for 24 h under control conditions (Fig. 2A, 0 Hz), at a pacing rate of 1 Hz and 3 Hz. 24 h pacing at 1 or 3 Hz led to a substantial decrease in  $I_{\text{CaL}}$  amplitude compared to non-paced control myocytes. Figure 2B shows average current–voltage ( $I$ – $V$ ) relations obtained from experiments similar to those shown in Fig. 2A. On average, pacing at 1 Hz decreased  $I_{\text{CaL}}$  amplitude by 31% from  $-8.6 \pm 0.3$  pApF $^{-1}$  ( $n = 74$ ) to  $5.9 \pm 0.3$  pApF $^{-1}$  ( $n = 56$ ,  $p < 0.001$ ,  $V_{\text{Pip}} = 0$  mV). A similar reduction in  $I_{\text{CaL}}$  amplitude ( $6.2 \pm 0.2$  pApF $^{-1}$ ,  $n = 48$ ,  $p < 0.001$ ,  $V_{\text{Pip}} = 0$  mV) was observed after pacing with 3 Hz. To address the question whether pacing altered single channel behavior of L-type  $\text{Ca}^{2+}$  channels, kinetic analysis was performed. Inactivation time constants of  $I_{\text{CaL}}$  are summarized in Table 3. 24 h pacing at 1 Hz led to small, but significant increase in  $\tau_1$  and  $\tau_2$  from  $18.3 \pm 0.5$  ms to  $20.7 \pm 0.8$  ms ( $p < 0.05$ ;  $V_{\text{Pip}} = 0$  mV) and from  $103 \pm 2.3$  ms to  $118 \pm 3.2$  ms ( $p < 0.001$ ), respectively. Moreover, the contribution of the short time constant  $\tau_1$  to total inactivation decreased from  $68.5 \pm 0.6\%$  to  $65.3 \pm 0.6\%$  ( $p < 0.001$ ). Similar results were obtained at a pacing rate of 3 Hz. Steady-state activation and steady-state inactivation are summarized in Fig. 3A. In control myocytes (0 Hz, black) half-maximal activation was observed at

**Table 2** Steady-state activation and inactivation parameters of  $I_{CaL}$  after 24–32 h primary culture

	$V_{50\text{ act}}$ (mV)	$k_{\text{act}}$ (mV)	$n_{\text{act}}$	$V_{50\text{ inac}}$ (mV)	$k_{\text{inac}}$ (mV)	$n_{\text{inac}}$
Control 0d	$-8.6 \pm 0.4$	$9.3 \pm 0.2$	68	$-33.4 \pm 0.4$	$-5.4 \pm 0.1$	111
Control 1d	$-12.8 \pm 0.6^*$	$8.1 \pm 0.2$	62	$-36.4 \pm 0.5^{***}$	$-6.2 \pm 0.1^{***}$	72

$V_{50\text{ act}}$  voltage at which half-maximal steady-state activation was observed,  $k_{\text{act}}$  slope factor of the steady-state activation curve,  $V_{50\text{ inac}}$  voltage at which half-maximal steady-state inactivation was observed,  $k_{\text{inac}}$  slope factor of the steady-state inactivation curve,  $n_{\text{act}}$  number of myocytes for steady-state activation,  $n_{\text{inac}}$  number of myocytes for steady-state inactivation

\* $p < 0.05$ , \*\*\* $p < 0.001$  vs. Control 0d

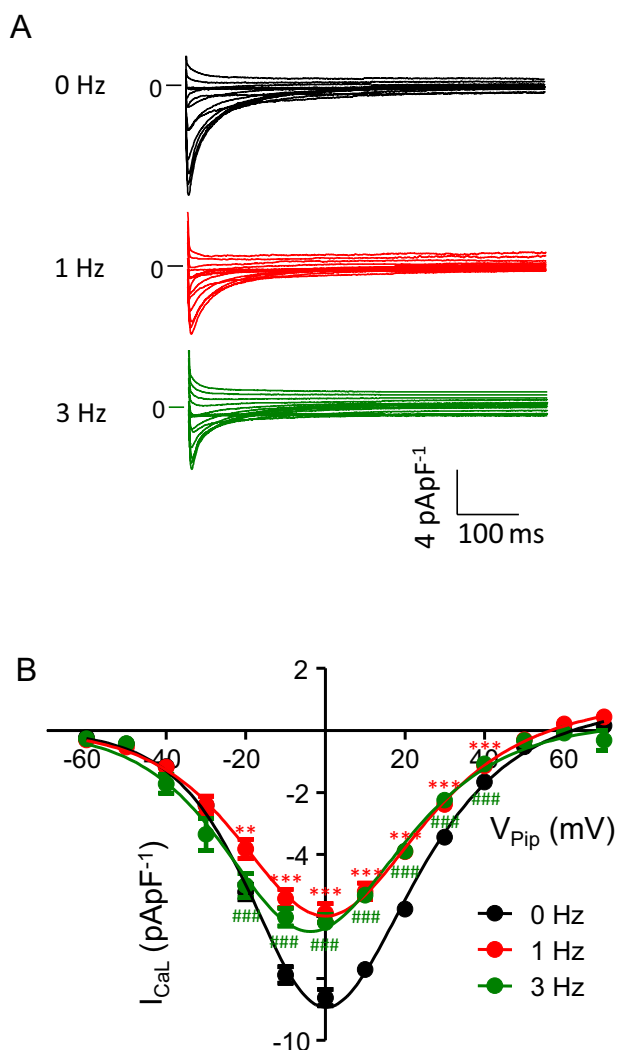


**Fig. 2** Pacing at 1 or 3 Hz decreases  $I_{CaL}$  density. **A** representative whole-cell current traces of  $I_{CaL}$  recorded from myocytes incubated for 24–32 h without pacing (black traces, '0 Hz') and with pacing at 1 Hz (red traces, '1 Hz') and at 3 Hz (green traces, '3 Hz'). **B** average current–voltage relations of currents similar to those shown in (A).  $I_{CaL}$  was quantified by subtracting the peak current from the current at the end of the voltage pulse (at 600 ms). Note that most error bars are smaller than the symbols.  $48 \leq n \leq 76$ . \*\* $p < 0.05$ , \*\*\* $p < 0.001$ , 1 Hz vs. 0 Hz. ### $p < 0.001$ , 3 Hz vs. 0 Hz

**Table 3** Inactivation time constant of  $I_{CaL}$  after pacing at 1 or 3 Hz

	n	$\tau 1$ (ms)	$\tau 2$ (ms)	% $\tau 1$ (%)	% $\tau 2$ (%)
0 Hz	73	$18.3 \pm 0.5$	$103 \pm 2.3$	$68.5 \pm 0.6$	$31.5 \pm 0.6$
1 Hz	57	$20.7 \pm 0.8^*$	$118 \pm 3.2^{***}$	$65.3 \pm 0.6^{***}$	$34.7 \pm 0.6^{***}$
3 Hz	52	$20.7 \pm 0.8^*$	$118 \pm 2.7^{***}$	$63.6 \pm 0.6^{***}$	$36.4 \pm 0.6^{***}$

$\tau 1$  and  $\tau 2$  inactivation time constants of  $I_{CaL}$  obtained by bi-exponentially fitting of current decay at  $V_{\text{pip}} = 0$  mV; %  $\tau 1$  and %  $\tau 2$  contribution of  $\tau 1$  and  $\tau 2$  to total inactivation (values are given in % of total inactivation),  $n$  number of myocytes

\* $p < 0.05$ , \*\*\* $p < 0.001$  vs. 0 Hz

$V_{50} = -15.3 \pm 0.4$  mV ( $n = 71$ ), while pacing with 1 Hz (red) and 3 Hz (green) significantly shifted half-maximal activation to more negative potentials of  $V_{50} = -17.5 \pm 0.7$  mV ( $n = 54$ ,  $p < 0.05$ ) and  $V_{50} = -19.3 \pm 1.0$  mV ( $n = 50$ ,  $p < 0.001$ ), respectively. The slope factor was not affected and averaged  $\sim 7.2$  mV (for detailed values see Table 4). In contrast, steady-state inactivation was only marginally affected by 1 Hz pacing with  $V_{50} = -35.5 \pm 0.5$  mV ( $n = 74$ , 0 Hz) and  $V_{50} = -33.6 \pm 0.5$  mV ( $n = 66$ , 1 Hz,  $p < 0.05$ ). Figure 3B summarizes the recovery from inactivation. Pacing at 1 Hz slightly but significantly shortened  $I_{CaL}$  recovery from  $\tau_{\text{rec}} = 140 \pm 3.6$  ms ( $n = 71$ ) to  $\tau_{\text{rec}} = 128 \pm 3.5$  ms ( $n = 67$ ,  $p < 0.05$ ) while 3 Hz pacing prolonged it to  $\tau_{\text{rec}} = 154 \pm 6.3$  ms ( $n = 51$ ,  $p < 0.05$ ).

### Incubation and Stimulation Alter mRNA Expression of Exon 1 and Exon 5 of *Cacna1c*

In an independent set of experiments, we then investigated the effect of 24 h incubation alone and of 24 h pacing at 1 Hz and 3 Hz on mRNA expression of the pore-forming  $\alpha$ -subunit of the cardiac L-type  $\text{Ca}^{2+}$  channel, *cacna1c*. After cell isolation, a fraction of myocytes was directly frozen for further processing, whereas the rest was either cultured under control conditions for 24 h (0 Hz) or subjected to continuous pacing for 24 h at 1 Hz or 3 Hz, after which the myocytes were frozen. For analysis of total *cacna1c* mRNA expression, we used specific intron-overspanning primers for exon 5, which is present in every splice variant and is therefore a useful marker for total *cacna1c* mRNA. Figure 4A summarizes exon 5 mRNA expression assessed

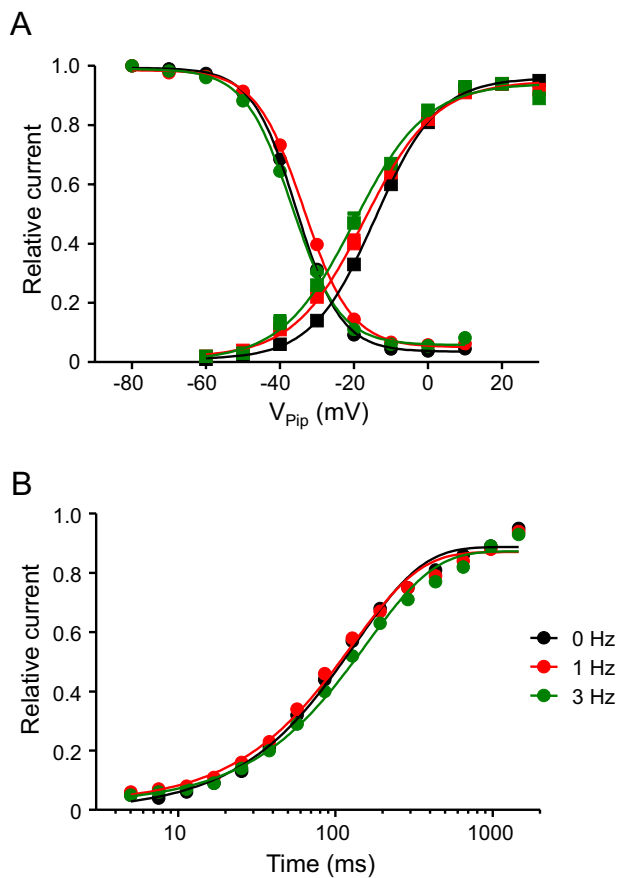


**Fig. 3** Pacing at 1 or 3 Hz alters  $I_{CaL}$  kinetics. **A** activation (circles) and steady-state inactivation (boxes) of  $I_{CaL}$  recorded from myocytes incubated for 24–32 h without pacing (black, ‘0 Hz’) and with pacing at 1 Hz (red, ‘1 Hz’) and at 3 Hz (green, ‘3 Hz’). **B** recovery from inactivation of  $I_{CaL}$  recorded from the groups mentioned above. For details regarding pulse protocols see methods section. Note that most error bars are smaller than the symbols.  $50 \leq n \leq 71$

by quantitative real-time RT-PCR and normalized to the expression level of exon 5 mRNA in freshly isolated myocytes. Incubation for 24 h under control conditions (0 Hz) led to a significant decrease in exon 5 mRNA expression to  $54.9 \pm 8.9\%$  ( $n=26$ ;  $p < 0.001$ ) of the level of freshly isolated cardiomyocytes. Pacing at 1 Hz and 3 Hz led to a further decrease in exon 5 mRNA expression down  $34.5 \pm 3.1\%$

( $n = 16$ ;  $p < 0.001$ ) and  $28.2 \pm 3.6\%$  ( $n = 10$ ;  $p < 0.001$ ), respectively. These results are qualitatively consistent with the decrease in  $I_{CaL}$  amplitude observed after 24 h incubation alone and the further decrease in  $I_{CaL}$  induced by pacing with 1 Hz or 3 Hz. We then asked if primary culture and pacing not only affect the total amount of *cacna1c* mRNA but also alter its isoform composition. Since especially splice variants of exon 1 are differentially expressed in cardiac myocytes, we addressed the expression of its three splice variants exon 1a, 1b and 1c using specific primers (see methods). Figure 4B shows that the expression of the cardiac specific variant of exon 1 decreased by 24 h primary culture under control conditions, a result which is similar to the decrease in expression of exon 5. Pacing at 1 or 3 Hz did not further alter the decrease in expression of exon 1a. In contrast, the expression of exon 1b and 1c (Fig. 4C, D), which is normally considerably lower than exon 1a expression in cardiac myocytes, significantly increased during 24 h incubation. This increase, however, was prevented by pacing at 1 or 3 Hz.

**Discussion**

In the present study we observed a small but significant decrease in  $I_{CaL}$  density of ~10% in isolated left ventricular myocytes after 24–36 h of primary culture. In previous reports, a substantial decrease (Mitcheson et al. 1996; Banyasz et al. 2008), an increase (Ellingsen et al. 1993) or no change (Yang et al. 2012) in  $I_{CaL}$  density in isolated cardiac myocytes after 24 h in primary culture have been reported. It is noteworthy that  $I_{CaL}$  density in primary culture is affected by hormones or growth factors often added to the culture medium such as corticosteroids (Bénitah and Vassort 1999; Wagner et al. 2008), thyroid hormones (Sunagawa et al. 2005; Yu et al. 2012), or insulin (Wacker et al. 2020). Therefore, culture conditions are important when interpreting spontaneous alterations of  $I_{CaL}$  density in primary culture. For example, Ellingsen et al. observed an increase in  $I_{CaL}$  density after 24 h of primary culture (Ellingsen et al. 1993) that was probably caused by the inclusion of T3 and insulin in the culture medium. Yang et al. (Yang et al. 2012) observed a rather constant  $I_{CaL}$  density over a period of up

**Table 4** Steady-state activation and inactivation parameters of  $I_{CaL}$  after pacing at 1 or 3 Hz

	$V_{50\ act}$ (mV)	$k_{act}$ (mV)	$n_{act}$	$V_{50\ inac}$ (mV)	$k_{inac}$ (mV)	$n_{inac}$
0 Hz	$-15.3 \pm 0.4$	$7.7 \pm 0.2$	71	$-35.5 \pm 0.5$	$-5.3 \pm 0.1$	74
1 Hz	$-17.5 \pm 0.7^*$	$8.2 \pm 0.4$	54	$-33.6 \pm 0.5$	$-6.0 \pm 0.1$	66
3 Hz	$-19.3 \pm 1.0^{***}$	$7.7 \pm 0.3$	50	$-36.6 \pm 0.5$	$-5.8 \pm 0.1$	57

$V_{50\ act}$  voltage at which half-maximal steady-state activation was observed,  $k_{act}$  slope factor of the steady-state activation curve,  $V_{50\ inac}$  voltage at which half-maximal steady-state inactivation was observed,  $k_{inac}$  slope factor of the steady-state inactivation curve,  $n_{act}$  number of myocytes for steady-state activation,  $n_{inac}$  number of myocytes for steady-state inactivation

\* $p < 0.05$ , \*\*\* $p < 0.001$  vs. 0 Hz

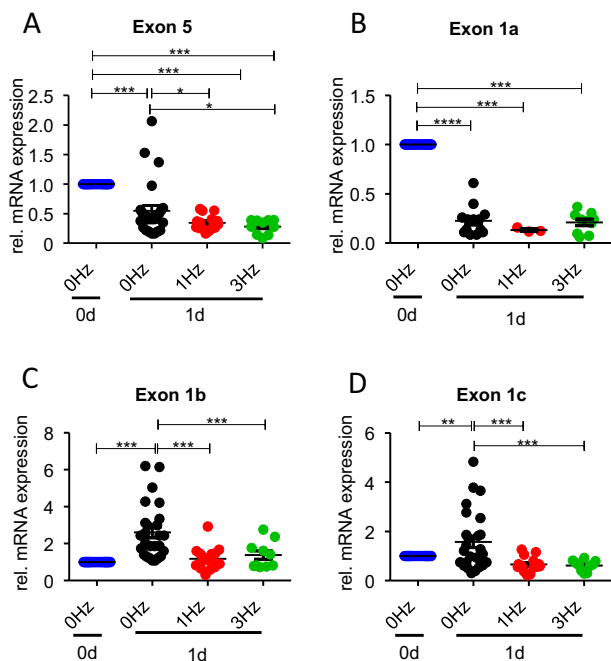


**Fig. 4** Effects of pacing on mRNA expression of total *cacnal1c* (exon 5) and exon 1 splice variants. **A** mRNA expression of exon 5 of freshly isolated myocytes (blue, 0 Hz, 0d) and of myocytes incubated for 24 h without pacing (black, 0 Hz, 1d) and with pacing at 1 Hz (red, 1 Hz, 1d) and at 3 Hz (green, 3 Hz, 1d).  $10 \leq n \leq 16$ . **B** mRNA expression of exon 1a in the same groups as in (A).  $3 \leq n \leq 16$ . **C** mRNA expression of exon 1b in the same groups as in (A).  $10 \leq n \leq 16$ . **D** mRNA expression of exon 1c in the same groups as in (A).  $10 \leq n \leq 16$ . mRNA expression was normalized to the level of freshly isolated myocytes (blue, 0 Hz, 0d) in each individual experiment. \* $p < 0.05$ , \*\* $p < 0.01$ , \*\*\* $p < 0.001$

to three days in isolated rabbit ventricular cardiomyocytes. However, they included 5% fetal bovine serum in the culture medium which contains, albeit at low concentrations, corticosteroids, IGF-1 and insulin, all well known to increase  $I_{CaL}$  density in primary culture (Bénitah and Vassort 1999; Wagner et al. 2008; Wacker et al. 2020). Using serum-free conditions without the addition of growth factors or hormones, Banyasz et al. (Banyasz et al. 2008) observed a substantial decrease of  $I_{CaL}$  of ~30% in isolated rat left ventricular cardiomyocytes within 24 h. In contrast to our study, they added taurine, creatine and l-carnitine to the culture medium which might have altered  $I_{CaL}$ . Taurine, for example, has been shown to in- or decrease  $I_{CaL}$  depending on the intracellular  $Ca^{2+}$  concentration in ventricular cardiomyocytes of the guinea pig (Sato and Horie 1997).

The mechanisms underlying the decline of  $I_{CaL}$  density in primary culture are unclear at the present. Banyasz et al. reported a decrease in density of the t-tubular system after 24 h of primary culture, which could account for a decrease in  $I_{CaL}$ , since a substantial fraction of L-type  $Ca^{2+}$  channels is located in the t-tubular system (Banyasz et al. 2008). In

a previous report, however, we did not observe a decrease in density of the t-tubular system after 24 h of primary culture under identical experimental conditions (Seidel et al. 2019), suggesting that other mechanisms underlie the small decrease in  $I_{CaL}$  density observed in the present study. Consistent with the decrease in  $I_{CaL}$  density we observed a decrease in total *cacnal1c* mRNA expression after 24 h in unstimulated primary culture. Since the number of L-type  $Ca^{2+}$  channels in the plasma membrane is a function of the rate of insertion of newly synthesized channels into the membrane and the net rate of retrieval of L-type  $Ca^{2+}$  channels from the membrane (Westhoff and Dixon 2021), a decrease in total *cacnal1c* mRNA expression could lead to decrease in the number of L-type  $Ca^{2+}$  channels in the plasma membrane within 24–36 h, provided that the channel half-life in the membrane is in an appropriate range. The half-life of L-type  $Ca^{2+}$  channels in the plasma membrane of cardiac myocytes is subject to complex regulation involving endosomal recycling of channels as well as pools of readily insertable  $CaV1.2$  that form an internal reservoir that can be inserted in the plasma membrane in certain conditions (Ito et al. 2019; del Villar et al. 2021). Using noco-dazole to stop trafficking of newly synthesized channels to the plasma membrane, channel half-life was estimated to be above 20 h in an immortalized atrial cell line (AT-1) (Conrad et al. 2018). In contrast, in freshly isolated mouse ventricular myocytes half-life was somewhat above 2 h only (del Villar et al. 2021). It is therefore safe to assume that the decrease in total *cacnal1c* mRNA expression after 24–36 h incubation caused the small decrease in  $I_{CaL}$  density.

In the present study, 24–36 h incubation had no effect on  $I_{CaL}$  inactivation and recovery from inactivation, however, steady-state activation and steady-state inactivation were shifted by a minor degree of 3–4 mV to more negative potentials. In another study using rat cardiomyocytes, no effect of primary culture on  $I_{CaL}$  kinetics was observed (Banyasz et al. 2008), however, our study included more than 60 myocytes per group, hence, the power to detect even minor differences in  $I_{CaL}$  kinetics was substantially larger in our study than e.g. in the study by Banyasz et al., which compared 7 myocytes per group. Similar results were obtained in rabbit cardiomyocytes (Mitcheson et al. 1996). The observed shift in steady-state activation and inactivation could result from several causes. Alterations in L-type channel phosphorylation at the N-terminal domain by Protein Kinase C for example (McHugh et al. 2000; Yang et al. 2005) during primary culture could account for the observed change. Alternatively, the composition of the underlying L-type  $Ca^{2+}$  channels might have changed. Indeed, we observed an increase in mRNA expression of the non-predominant exon 1b and exon 1c after 24 h incubation. Since exon 1b and exon 1c are also expressed in smooth muscle cells (Cheng et al. 2007) and potentially also in fibroblasts (Chen et al. 2010), the



increase in exon 1b + c expression during 24 h primary culture might be secondary to proliferation of smooth muscle cells or fibroblast that may be present in the cardiomyocyte culture. However, in control experiments we found that the mRNA expression of vimentin and DDR2, both markers for smooth muscle cells and fibroblasts (Camelliti et al. 2005), decreased during 24 h primary culture (data not shown). This suggests that the increase in mRNA expression of exon 1b + c after 24 h incubation most likely results from a decrease in their expression in cardiomyocytes. While an early study did not detect significant differences in steady-state activation or inactivation between the cardiac and the vascular variant of Cav1.2 (Hu and Marban 1998), Bartels et al. (Bartels et al. 2018) more recently showed in an elegant study, that replacing exon 1a by exon 1b leads to a shift of steady-state activation and inactivation towards more negative potentials by 3–4 mV. Since L-type  $\text{Ca}^{2+}$  channels composed of exon 1c display similar steady-state activation and inactivation as  $\text{Ca}^{2+}$  channels containing exon 1b (Cheng et al. 2007), one could speculate that the small shift in steady-state activation and inactivation potentials originates from an increased contribution of  $\text{Ca}^{2+}$  channels containing exon 1b or exon 1c instead of exon 1a.

Taken together, we have identified serum-free culture conditions under which  $I_{\text{CaL}}$  density remains rather constant and is therefore suitable for experiments addressing medium to long term effects over a period of 24–36 h on  $I_{\text{CaL}}$ .

Pacing at 1 or 3 Hz for 24–36 h substantially decreased  $I_{\text{CaL}}$  density as well as total *cacna1c* mRNA expression compared to non-paced controls incubated under identical conditions. This is in line with observations in a canine model of atrial fibrillation induced by rapid pacing for 1, 7, and 42 days in which a continuous decrease in  $I_{\text{CaL}}$  density in atrial cardiomyocytes was observed over the period investigated (Yue et al. 1997) as well as a decrease in mRNA expression of *cacna1c* (Yue et al. 1999). Similar results were obtained in rabbits upon rapid ventricular pacing for 24 h which led to a decrease in  $I_{\text{CaL}}$  density and *cacna1c* mRNA expression (Bosch et al. 2003). Moreover, 3 Hz pacing of isolated canine atrial myocytes for 24 h decreased  $I_{\text{CaL}}$  density by 55%, while 1 Hz pacing did not (Satin et al. 2011). In contrast, in isolated rat cardiac myocytes, an increase in  $I_{\text{CaL}}$  has been reported after 48 h of 3 Hz pacing (Berger et al. 1994). However, in this study, myocytes were incubated with different hormones and substances known to alter  $I_{\text{CaL}}$  such as T3, insulin, creatine and taurine and, using identical culture conditions, the same group also observed an increase in  $I_{\text{CaL}}$  by incubation alone (Ellingsen et al. 1993). It is therefore conceivable that the increase in  $I_{\text{CaL}}$  they observed is at least related to the presence of the aforementioned substances.

Pacing of isolated cardiomyocytes in primary culture resembles the regular electrical excitation the myocytes

experience in vivo. The contractile response, however, differs. Individual myocytes in a culture dish contract freely without any extra load (so-called unloaded cell shortening), so they only generate the force necessary to alter their shape from the relaxed to the contracted form. This force is far less compared to the force developed in vivo. Therefore, one could consider the decrease in  $I_{\text{CaL}}$  density as a response to unloaded regular contractions. A comparable in vivo condition has been achieved in rats by transplanting a donor heart to the abdominal aorta of a recipient animal, where it receives coronary perfusion and contracts regularly without ventricular filling or a stroke volume over a long time (up to several weeks). Unloaded hearts develop a significant atrophy and undergo several changes in electrophysiology,  $\text{Ca}^{2+}$  cycling, contractility and gene expression (Schwoerer et al. 2008, 2013; El-Armouche et al. 2010). However,  $I_{\text{CaL}}$  density was not affected (Ibrahim et al. 2010) after 2 weeks or even increased (Schwoerer et al. 2008) after four weeks of cardiac unloading, suggesting that the decrease in  $I_{\text{CaL}}$  density caused by pacing of isolated myocytes in primary culture may not directly be related to cardiac atrophy. Instead, there is evidence, that pacing of isolated myocytes at 3 Hz might even lead to a hypertrophic response as it increased the rate of phenylalanine incorporation, total cellular protein content, and cell size (Kaye et al. 1996). Depending on etiology, duration and other factors, cardiac hypertrophy can exert different effects on  $I_{\text{CaL}}$  including an increase, no change or a decrease of  $I_{\text{CaL}}$  density (Volk and Ehmke 2002). Nevertheless, a more recent study showed that a decrease in  $I_{\text{CaL}}$  density can lead to hypertrophy (Goonasekera et al. 2012). Taken together, the observed decrease in  $I_{\text{CaL}}$  density in the present study can be considered as part of a hypertrophic response induced by pacing, however, further experiments need to address this hypothesis.

Cardiomyocyte pacing could also indirectly alter  $I_{\text{CaL}}$  density via affecting the density of the t-tubular system. Loss or alterations in the t-tubular system are a common phenomenon in heart failure with reduced ejection fraction, independent of its etiology, and the t-tubular system has the potential to recover, if the noxious stimulus is removed (Setterberg et al. 2021). Interestingly, pacing rate and rhythm might also affect the t-tubular system. T-system recovery has been observed in a canine model of dysynchronous heart failure, when regular biventricular pacing was applied (Sachse et al. 2012). Moreover, the regularity of pacing might also be important, since heart failure associated alterations in the t-tubular system could be reversed by reinstating heart rate variability in a goat model of heart failure (Shanks et al. 2022). We therefore cannot exclude that potential pacing-induced changes of the t-tubular system might have contributed to the observed changes in  $I_{\text{CaL}}$ .

Pacing with 1 or 3 Hz led to minor alterations in  $I_{\text{CaL}}$  kinetics. Both, the fast and the slow inactivation time

contents  $\tau_1$  and  $\tau_2$  increased. Since especially the fast inactivation of  $I_{CaL}$  is mediated by  $Ca^{2+}$  entering through the open channels (Hadley and Hume 1987), the increase of  $\tau_1$  might be secondary to the substantial decrease in  $I_{CaL}$  density after 24–32 h of 1 or 3 Hz pacing. Moreover, pacing significantly shifted steady-state activation to more negative potentials while steady-state inactivation was only marginally affected. Similar to the effect of incubation alone, this could be a result of a relative decrease of the expression of exon 1a compared to exon 1b and exon 1c observed after pacing. Recovery from inactivation did not follow a clear pattern, pacing at 1 Hz led to a mild decrease while pacing at 3 Hz lead to a mild increase in the recovery time constant.

**Acknowledgements** We gratefully acknowledge the expert technical assistance of Céline Grüninger and Lorenz McCargo.

**Author Contributions** TV, TR, and ER contributed to the conception and design. TR, ER, and SN contributed to the data acquisition and experiments. TV, AR, TR, ER, and SN contributed to the data analysis. TV, AR, and TR contributed to the interpretation of the data. AR and TV drafted the manuscript. All authors critically revised and approved the manuscript.

**Funding** Open Access funding enabled and organized by Projekt DEAL. The authors did not receive support from any organization for the submitted work. The authors have no relevant financial or non-financial interests to disclose.

**Data Availability** The datasets generated during and/or analysed during the current study are available from the corresponding author on reasonable request.

## Declarations

**Conflict of interest** The authors have no conflicts of interest to declare that are relevant to the content of this article.

**Open Access** This article is licensed under a Creative Commons Attribution 4.0 International License, which permits use, sharing, adaptation, distribution and reproduction in any medium or format, as long as you give appropriate credit to the original author(s) and the source, provide a link to the Creative Commons licence, and indicate if changes were made. The images or other third party material in this article are included in the article's Creative Commons licence, unless indicated otherwise in a credit line to the material. If material is not included in the article's Creative Commons licence and your intended use is not permitted by statutory regulation or exceeds the permitted use, you will need to obtain permission directly from the copyright holder. To view a copy of this licence, visit <http://creativecommons.org/licenses/by/4.0/>.

## References

- Abernethy DR, Soldatov NM (2002) Structure-functional diversity of human L-type  $Ca^{2+}$  channel: perspectives for new pharmacological targets. *J Pharmacol Exp Ther* 300(3):724–728. <https://doi.org/10.1124/jpet.300.3.724>
- Banyasz T, Lozinskiy I, Payne CE, Edelmann S, Norton B, Chen B, Chen-Izu Y, Izu LT, Balke CW (2008) Transformation of adult rat cardiac myocytes in primary culture. *Exp Physiol* 93(3):370–382. <https://doi.org/10.1113/expphysiol.2007.040659>
- Barnett DW, Pressel DM, Misler S (1995) Voltage-dependent  $Na^{+}$  and  $Ca^{2+}$  currents in human pancreatic islet  $\beta$ -cells: evidence for roles in the generation of action potentials and insulin secretion. *Pflügers Archiv Euro J Physiol* 431(2):272–282. <https://doi.org/10.1007/BF00410201>
- Bartels P, Yu D, Huang H, Hu Z, Herzig S, Soong TW (2018) Alternative splicing at N terminus and domain I modulates  $CaV1.2$  inactivation and surface expression. *Biophys J* 114(9):2095–2106. <https://doi.org/10.1016/j.bpj.2018.03.029>
- Bénitah JP, Vassort G (1999) Aldosterone upregulates  $Ca^{2+}$  current in adult rat cardiomyocytes. *Circ Res* 85(12):1139–1145. <https://doi.org/10.1161/01.RES.85.12.1139>
- Berger SM, Bartsch D (2014) The role of L-type voltage-gated calcium channels  $CaV1.2$  and  $CaV1.3$  in normal and pathological brain function. *Cell Tissue Res* 357(2):463–476. <https://doi.org/10.1007/s00441-014-1936-3>
- Berger HJ, Prasad SK, Davidoff AJ, Pimental D, Ellingsen O, Marsh JD, Smith TW, Kelly RA (1994) Continual electric field stimulation preserves contractile function of adult ventricular myocytes in primary culture. *Am J Physiol Heart Circ Physiol*. <https://doi.org/10.1152/ajpheart.1994.266.1.h341>
- Biel M, Hullin R, Freundner S, Singer D, Dascal N, Flockerzi V, Hofmann F (1991) Tissue-specific expression of high-voltage-activated dihydropyridine-sensitive L-type calcium channels. *Eur J Biochem* 200(1):81–88. <https://doi.org/10.1111/j.1432-1033.1991.tb21051.x>
- Bodi I, Mikala G, Koch SE, Akhter SA, Schwartz A (2005) The L-type calcium channel in the heart: the beat goes on. *J Clin Invest* 115(12):3306–3317. <https://doi.org/10.1172/JCI27167>
- Bosch RF, Scherer CR, Rüb N, Wöhrl S, Steinmeyer K, Haase H, Busch AE, Seipel L, Kühlkamp V (2003) Molecular mechanisms of early electrical remodeling: transcriptional down-regulation of ion channel subunits reduces  $ICa$ ,  $I_L$  and  $I_{to}$  in rapid atrial pacing in rabbits. *J Am Coll Cardiol* 41(5):858–869. [https://doi.org/10.1016/S0735-1097\(02\)02922-4](https://doi.org/10.1016/S0735-1097(02)02922-4)
- Brandt A, Striessnig J, Moser T (2003)  $CaV1.3$  channels are essential for development and presynaptic activity of cochlear inner hair cells. *J Neurosci* 23(34):10832–10840. <https://doi.org/10.1523/jneurosci.23-34-10832.2003>
- Calin-Jageman I, Lee A (2008)  $CaV1$  L-type  $Ca^{2+}$  channel signaling complexes in neurons. *J Neurochem* 105(3):573–583. <https://doi.org/10.1111/j.1471-4159.2008.05286.x>
- Camelliti P, Borg TK, Kohl P (2005) Structural and functional characterisation of cardiac fibroblasts. *Cardiovasc Res* 65(1):40–51. <https://doi.org/10.1016/J.CARDIORES.2004.08.020>
- Chen JB, Tao R, Sun HY, Tse HF, Lau CP, Li GR (2010) Multiple  $Ca^{2+}$  signaling pathways regulate intracellular  $Ca^{2+}$  activity in human cardiac fibroblasts. *J Cell Physiol* 223(1):68–75. <https://doi.org/10.1002/JCP.22010>
- Cheng X, Liu J, Asuncion-Chin M, Blaskova E, Bannister JP, Dopico AM, Jaggar JH (2007) A novel  $Ca(V)1.2$  N terminus expressed in smooth muscle cells of resistance size arteries modifies channel regulation by auxiliary subunits. *J Biol Chem* 282(40):29211–29221. <https://doi.org/10.1074/jbc.M610623200>
- Chen-Izu Y, Chen L, Bányász T, McCulle SL, Norton B, Scharf SM, Agarwal A, Patwardhan A, Izu LT, Balke CW (2007) Hypertension-induced remodeling of cardiac excitation-contraction coupling in ventricular myocytes occurs prior to hypertrophy development. *Am J Physiol Heart Circ Physiol* 293(6):H3301–H3310. <https://doi.org/10.1152/ajpheart.00259.2007>
- Conrad R, Stölting G, Hendriks J, Ruello G, Kortzak D, Jordan N, Gensch T, Hidalgo P (2018) Rapid turnover of the cardiac L-type  $Ca V 12$  channel by endocytic recycling regulates its cell surface

- availability. *iScience* 7:1–15. <https://doi.org/10.1016/J.ISCI.2018.08.012>
- Coraboeuf E, Nargeot J (1993) Electrophysiology of human cardiac cells. *Cardiovasc Res* 27(10):1713–1725. <https://doi.org/10.1093/cvr/27.10.1713>
- del Villar SG, Voelker TL, Westhoff M, Reddy GR, Spooner HC, Navedo MF, Dickson EJ, Dixon RE (2021)  $\beta$ -Adrenergic control of sarcolemmal CaV1.2 abundance by small GTPase Rab proteins. *Proc Natl Acad Sci USA*. <https://doi.org/10.1073/PNAS.2017937118/-DCSUPPLEMENTAL>
- Dewenter M, Von Der Lieth A, Katus HA, Backs J (2017) Calcium signaling and transcriptional regulation in cardiomyocytes. *Circ Res* 121(8):1000–1020. <https://doi.org/10.1161/CIRCRESAHA.117.310355>
- Eisner DA, Caldwell JL, Kistamás K, Trafford AW (2017) Calcium and excitation-contraction coupling in the heart. *Circ Res* 121(2):181–195. <https://doi.org/10.1161/CIRCRESAHA.117.3.10230>
- El-Armouche A, Schwoerer AP, Neuber C, Emmons J, Biermann D, Christalla T, Grundhoff A, Eschenhagen T, Zimmermann WH, Ehmke H (2010) Common MicroRNA signatures in cardiac hypertrophic and atrophic remodeling induced by changes in hemodynamic load. *PLoS ONE*. <https://doi.org/10.1371/journal.pone.0014263>
- Ellingsen O, Davidoff AJ, Prasad SK, Berger HJ, Springhorn JP, Marsh JD, Kelly RA, Smith TW (1993) Adult rat ventricular myocytes cultured in defined medium: phenotype and electromechanical function. *Am J Physiol Heart Circ Physiol*. <https://doi.org/10.1152/ajpheart.1993.265.2.h747>
- Feng T, Kalyaanamoorthy S, Barakat K (2018) L-type calcium channels: Structure and functions. *Ion Channels Health Sickness*. <https://doi.org/10.5772/intechopen.77305>
- Fischer C, Milting H, Fein E, Reiser E, Lu K, Seidel T, Schinner C, Schwarzmayr T, Schramm R, Tomasi R, Husse B, Cao-Ehlker X, Pohl U, Dendorfer A (2019) Long-term functional and structural preservation of precision-cut human myocardium under continuous electromechanical stimulation in vitro. *Nat Commun*. <https://doi.org/10.1038/s41467-018-08003-1>
- Foltz WU, Wagner M, Rudakova E, Volk T (2012) N-acetylcysteine prevents electrical remodeling and attenuates cellular hypertrophy. *Basic Res Cardiol*. <https://doi.org/10.1007/s00395-012-0290-4>
- Gambardella J, Trimarco B, Iaccarino G, Santulli G (2018) New insights in cardiac calcium handling and excitation-contraction coupling. *Adv Exp Med Biol* 1067:373–385. [https://doi.org/10.1007/5584\\_2017\\_106](https://doi.org/10.1007/5584_2017_106)
- Goonasekera SA, Hammer K, Auger-Messier M, Bodi I, Chen X, Zhang H, Reiken S, Elrod JW, Correll RN, York AJ, Sargent MA, Hofmann F, Moosmang S, Marks AR, Houser SR, Bers DM, Molkenkin JD (2012) Decreased cardiac L-type Ca<sup>2+</sup> channel activity induces hypertrophy and heart failure in mice. *J Clin Investig* 122(1):280–290. <https://doi.org/10.1172/JCI58227>
- Hadley RW, Hume JR (1987) An intrinsic potential-dependent inactivation mechanism associated with calcium channels in guinea-pig myocytes. *J Physiol* 389(1):205–222. <https://doi.org/10.1113/JPHYSIOL.1987.SP016654>
- Hirt MN, Boeddinghaus J, Mitchell A, Schaaf S, Börnchen C, Müller C, Schulz H, Hubner N, Stenzig J, Stoehr A, Neuber C, Eder A, Luther PK, Hansen A, Eschenhagen T (2014) Functional improvement and maturation of rat and human engineered heart tissue by chronic electrical stimulation. *J Mol Cell Cardiol* 74:151–161. <https://doi.org/10.1016/j.yjmcc.2014.05.009>
- Hofmann F, Flockerzi V, Kahl S, Wegener JW (2014) L-type CaV12 calcium channels: from in vitro findings to in vivo function. *Physiol Rev* 94(1):303–326. <https://doi.org/10.1152/physrev.00016.2013>
- Hu H, Marban E (1998) Isoform-specific inhibition of L-type calcium channels by dihydropyridines is independent of isoform-specific gating properties. *Mol Pharmacol* 53(5):1–10
- Ibrahim M, Masri AA, Navaratnarajah M, Siedlecka U, Soppa GK, Moshkov A, Al-Saud SA, Gorelik J, Yacoub MH, Terracciano CMN (2010) Prolonged mechanical unloading affects cardiomyocyte excitation-contraction coupling, transverse-tubule structure, and the cell surface. *FASEB J* 24(9):3321–3329. <https://doi.org/10.1096/FJ.10-156638>
- Ito DW, Hannigan KI, Ghosh D, Xu B, del Villar SG, Xiang YK, Dickson EJ, Navedo MF, Dixon RE (2019)  $\beta$ -adrenergic-mediated dynamic augmentation of sarcolemmal Ca V 1.2 clustering and co-operativity in ventricular myocytes. *J Physiol* 597(8):2139–2162. <https://doi.org/10.1113/JP277283>
- Kaye D, Pimental D, Prasad S, Mäki T, Berger HJ, McNeil PL, Smith TW, Kelly RA (1996) Role of transiently altered sarcolemmal membrane permeability and basic fibroblast growth factor release in the hypertrophic response of adult rat ventricular myocytes to increased mechanical activity in vitro. *J Clin Investig* 97(2):281–291. <https://doi.org/10.1172/JCI118414>
- Kim JC, Le QA, Woo SH (2020) Alterations of Ca<sup>2+</sup> signaling and Ca<sup>2+</sup> release sites in cultured ventricular myocytes with intact internal Ca<sup>2+</sup> storage. *Biochem Biophys Res Commun* 527(2):379–386. <https://doi.org/10.1016/j.bbrc.2020.04.059>
- Lee A, Wang S, Williams B, Hagen J, Scheetz TE, Haeseleer F (2015) Characterization of Ca v 1.4 complexes ( $\alpha$  1.4,  $\beta$  2, and  $\alpha$  2  $\delta$  4) in HEK293T cells and in the retina. *J Biol Chem* 290(3):1505–1521. <https://doi.org/10.1074/jbc.M114.607465>
- Liao P, Tan FY, Mui CL, Yue DT, Tuck WS (2005) Splicing for alternative structures of Cav1.2 Ca<sup>2+</sup> channels in cardiac and smooth muscles. *Cardiovasc Res* 68(2):197–203. <https://doi.org/10.1016/j.cardiores.2005.06.024>
- Linz KW, Meyer R (2000) Profile and kinetics of L-type calcium current during the cardiac ventricular action potential compared in guinea-pigs, rats and rabbits. *Pflügers Archiv Euro J Physiol* 439(5):588–599. <https://doi.org/10.1007/s004249900212>
- Lipscombe D, Andrade A (2015) Calcium channel CaV $\alpha$ 1 splice isoforms—tissue specificity and drug action. *Curr Mol Pharmacol* 8(1):22–31. <https://doi.org/10.2174/1874467208666150507103215>
- Marcantoni A, Baldelli P, Hernandez-Guijo JM, Comunanza V, Carabelli V, Carbone E (2007) L-type calcium channels in adrenal chromaffin cells: role in pace-making and secretion. *Cell Calcium* 42(4–5):397–408. <https://doi.org/10.1016/j.ceca.2007.04.015>
- McHugh D, Sharp EM, Scheuer T, Catterall WA (2000) Inhibition of cardiac L-type calcium channels by protein kinase C phosphorylation of two sites in the N-terminal domain. *Proc Natl Acad Sci* 97(22):12334–12338. <https://doi.org/10.1073/pnas.210384297>
- Michna M, Knirsch M, Hoda JC, Muenkner S, Langer P, Platzer J, Striessnig J, Engel J (2003) Cav 1.3 ( $\alpha$ 1D) Ca<sup>2+</sup> currents in neonatal outer hair cells of mice. *J Physiol* 553(3):747–758. <https://doi.org/10.1113/jphysiol.2003.053256>
- Mitcheson JS, Hancox JC, Levi AJ (1996) Action potentials, ion channel currents and transverse tubule density in adult rabbit ventricular myocytes maintained for 6 days in cell culture. *Pflügers Archiv Euro J Physiol* 431(6):814–827. <https://doi.org/10.1007/s004240050073>
- Moosmang S, Schulla V, Welling A, Feil R, Feil S, Wegener JW, Hofmann F, Klugbauer N (2003) Dominant role of smooth muscle L-type calcium channel Cav1.2 for blood pressure regulation. *EMBO J* 22(22):6027–6034. <https://doi.org/10.1093/EMBOJ/CDG583>
- Muth JN, Bodi I, Lewis W, Varadi G, Schwartz A (2001) A Ca<sup>2+</sup>-dependent transgenic model of cardiac hypertrophy. *Circulation* 103(1):140–147. <https://doi.org/10.1161/01.CIR.103.1.140>



- Nitert MD, Nagorny CLF, Wendt A, Eliasson L, Mulder H (2008) Cav1.2 rather than Cav1.3 is coupled to glucose-stimulated insulin secretion in INS-1 832/13 cells. *J Mol Endocrinol* 41(1–2):1–11. <https://doi.org/10.1677/JME-07-0133>
- Nunes SS, Miklas JW, Liu J, Aschar-Sobbi R, Xiao Y, Zhang B, Jiang J, Massé S, Gagliardi M, Hsieh A, Thavandiran N, Laflamme MA, Nanthakumar K, Gross GJ, Backx PH, Keller G, Radisic M (2013) Biowire: a platform for maturation of human pluripotent stem cell-derived cardiomyocytes. *Nat Methods* 10(8):781–787. <https://doi.org/10.1038/nmeth.2524>
- Parameswaran S, Kumar S, Verma RS, Sharma RK (2013) Cardiomyocyte culture—an update on the in vitro cardiovascular model and future challenges. *Can J Physiol Pharmacol* 91(12):985–998. <https://doi.org/10.1139/cjpp-2013-0161>
- Ruan JL, Tulloch NL, Razumova MV, Saiget M, Muskheili V, Pabon L, Reinecke H, Regnier M, Murry CE (2016) Mechanical stress conditioning and electrical stimulation promote contractility and force maturation of induced pluripotent stem cell-derived human cardiac tissue. *Circulation* 134(20):1557–1567. <https://doi.org/10.1161/CIRCULATIONAHA.114.014998>
- Sachse FB, Torres NS, Savio-Galimberti E, Aiba T, Kass DA, Tomaselli GF, Bridge JH (2012) Subcellular structures and function of myocytes impaired during heart failure are restored by cardiac resynchronization therapy. *Circ Res* 110(4):588–597. <https://doi.org/10.1161/CIRCRESAHA.111.257428>
- Satin J, Schroder EA, Crump SM (2011) L-type calcium channel auto-regulation of transcription. *Cell Calcium*. <https://doi.org/10.1016/j.ceca.2011.01.001>
- Satoh H, Horie M (1997) Actions of taurine on the L-type Ca<sup>2+</sup> channel current in Guinea pig ventricular cardiomyocytes. *J Cardiovasc Pharmacol* 30(6):711–716. <https://doi.org/10.1097/00005344-199712000-00002>
- Schoenmakers T, Visser GJ, Flik G, Theuvenet A (1992) CHELATOR: an improved method for computing metal ion concentrations in physiological solutions. *Biotechniques* 4:1–8
- Schwoerer AP, Melnychenko I, Goltz D, Hedinger N, Broichhausen I, El-Armouche A, Eschenhagen T, Volk T, Ehmke H (2008) Unloaded rat hearts in vivo express a hypertrophic phenotype of cardiac repolarization. *J Mol Cell Cardiol* 45(5):633–641. <https://doi.org/10.1016/j.yjmcc.2008.02.271>
- Schwoerer AP, Neef S, Broichhausen I, Jacubeit J, Tiburcy M, Wagner M, Biermann D, Didié M, Vettel C, Maier LS, Zimmermann WH, Carrier L, Eschenhagen T, Volk T, El-Armouche A, Ehmke H (2013) Enhanced Ca<sup>2+</sup> influx through cardiac L-type Ca<sup>2+</sup> channels maintains the systolic Ca<sup>2+</sup> transient in early cardiac atrophy induced by mechanical unloading. *Pflügers Archiv Euro J Physiol* 465(12):1763–1773. <https://doi.org/10.1007/s00424-013-1316-y>
- Seidel T, Fiegle DJ, Baur TJ, Ritzer A, Nay S, Heim C, Weyand M, Milting H, Oakley RH, Cidlowski JA, Volk T (2019) Glucocorticoids preserve the t-tubular system in ventricular cardiomyocytes by upregulation of autophagic flux. *Basic Res Cardiol*. <https://doi.org/10.1007/s00395-019-0758-6>
- Setterberg IE, Le C, Frisk M, Li J, Louch WE (2021) The physiology and pathophysiology of T-tubules in the heart. *Front Physiol*. <https://doi.org/10.3389/fphys.2021.718404>
- Shanks J, Abukar Y, Lever NA, Pachen M, LeGrice IJ, Crossman DJ, Nogaret A, Paton JFR, Ramchandra R (2022) Reverse re-modelling chronic heart failure by reinstating heart rate variability. *Basic Res Cardiol*. <https://doi.org/10.1007/S00395-022-00911-0>
- Snutch TP, Tomlinson WJ, Leonard JP, Gilbert MM (1991) Distinct calcium channels are generated by alternative splicing and are differentially expressed in the mammalian CNS. *Neuron* 7(1):45–57. [https://doi.org/10.1016/0896-6273\(91\)90073-9](https://doi.org/10.1016/0896-6273(91)90073-9)
- Sunagawa M, Yamakawa M, Shimabukuro M, Higa N, Takasu N, Kosugi T (2005) Electrophysiologic characteristics of atrial myocytes in levo-thyroxine-treated rats. *Thyroid* 15(1):3–11. <https://doi.org/10.1089/thy.2005.15.3>
- Tang ZZ, Liang MC, Lu S, Yu D, Yu CY, Yue DT, Soong TW (2004) Transcript scanning reveals novel and extensive splice variations in human I-type voltage-gated calcium channel, Cav1.2 alpha1 subunit. *J Biol Chem* 279(43):44335–44343. <https://doi.org/10.1074/jbc.M407023200>
- Tseng TT, McMahan AM, Zahm RJ, Pacold ME, Jakobsson E (2006) Calcium channel auxiliary subunits. *J Mol Microbiol Biotechnol* 11(6):326–344. <https://doi.org/10.1159/000095635>
- Vandael DHF, Mahapatra S, Calorio C, Marcantoni A, Carbone E (2013) Cav1.3 and Cav1.2 channels of adrenal chromaffin cells: emerging views on cAMP/cGMP-mediated phosphorylation and role in pacemaking. *Biochim Biophys Acta—Biomembr* 1828(7):1608–1618. <https://doi.org/10.1016/j.bbmem.2012.11.013>
- Volk T, Ehmke H (2002) Conservation of L-type Ca<sup>2+</sup> current characteristics in endo- and epicardial myocytes from rat left ventricle with pressure-induced hypertrophy. *Pflügers Archiv Euro J Physiol* 443(3):399–404. <https://doi.org/10.1007/S004240100712>
- Wacker C, Dams N, Schauer A, Ritzer A, Volk T, Wagner M (2020) Region-specific mechanisms of corticosteroid-mediated inotropy in rat cardiomyocytes. *Sci Rep*. <https://doi.org/10.1038/s41598-020-68308-4>
- Wagner M, Rudakova E, Volk T (2008) Aldosterone-induced changes in the cardiac L-type Ca<sup>2+</sup> current can be prevented by antioxidants in vitro and are absent in rats on low salt diet. *Pflügers Archiv Euro J Physiol* 457(2):339–349. <https://doi.org/10.1007/s00424-008-0518-1>
- Wagner M, Riepe KG, Eberhardt E, Volk T (2010) Open channel block of the fast transient outward K<sup>+</sup> current by primaquine and chlo-roquine in rat left ventricular cardiomyocytes. *Eur J Pharmacol* 647(1–3):13–20. <https://doi.org/10.1016/J.EJPHAR.2010.08.007>
- Wang D, Papp AC, Binkley PF, Johnson JA, Sadée W (2006) Highly variable mRNA expression and splicing of L-type voltage-dependent calcium channel alpha subunit 1C in human heart tissues. *Pharmacogenet Genomics* 16(10):735–745. <https://doi.org/10.1097/01.fpc.0000230119.34205.8a>
- Westhoff M, Dixon RE (2021) Mechanisms and regulation of cardiac Cav1.2 trafficking. *Int J Mol Sci*. <https://doi.org/10.3390/IJMS2115927>
- Wu J, Yan N, Yan Z (2017) Structure-function relationship of the voltage-gated calcium channel Cav1.1 complex. *Adv Exp Med Biol* 981:23–39. [https://doi.org/10.1007/978-3-319-55858-5\\_2](https://doi.org/10.1007/978-3-319-55858-5_2)
- Yang L, Liu G, Zakharov SI, Morrow JP, Rybin VO, Steinberg SF, Marx SO (2005) Ser 1928 is a common site for Cav1.2 phosphorylation by protein kinase C isoforms. *J Biol Chem* 280(1):207–214. <https://doi.org/10.1074/jbc.M410509200>
- Yang X, Chen G, Papp R, Defranco DB, Zeng F, Salama G (2012) Oestrogen upregulates L-type Ca<sup>2+</sup> channels via oestrogen-receptor- $\alpha$  by a regional genomic mechanism in female rabbit hearts. *J Physiol* 590(3):493–508. <https://doi.org/10.1113/jphysiol.2011.219501>
- Yu Z, Wang T, Xu L, Huang CX (2012) Thyroid hormone increased L-type calcium channel mRNA expression and L-type calcium current of myocytes in rabbits. *Bio-Med Mater Eng* 22(1–3):49–55. <https://doi.org/10.3233/BME-2012-0689>
- Yue L, Feng J, Gaspo R, Li GR, Wang Z, Nattel S (1997) Ionic remodeling underlying action potential changes in a canine model of atrial fibrillation. *Circ Res* 81(4):512–525. <https://doi.org/10.1161/01.RES.81.4.512>
- Yue L, Melnyk P, Gaspo R, Wang Z, Nattel S (1999) Molecular mechanisms underlying ionic remodeling in a dog model of atrial fibrillation. *Circ Res* 84(7):776–784. <https://doi.org/10.1161/01.RES.84.7.776>
- Zamponi GW, Striessnig J, Koschak A, Dolphin AC (2015) The physiology, pathology, and pharmacology of voltage-gated calcium

channels and their future therapeutic potential. *Pharmacol Rev* 67(4):821–870. <https://doi.org/10.1124/pr.114.009654>

Zhang X, Ai X, Nakayama H, Chen B, Harris DM, Tang M, Xie Y, Szeto C, Li Y, Li Y, Zhang H, Eckhart AD, Koch WJ, Molkentin JD, Chen X (2016) Persistent increases in Ca<sup>2+</sup> influx through Cav1.2 shortens action potential and causes Ca<sup>2+</sup> overload-induced afterdepolarizations and arrhythmias. *Basic Res Cardiol* 111(1):1–16. <https://doi.org/10.1007/s00395-015-0523-4>

**Publisher's Note** Springer Nature remains neutral with regard to jurisdictional claims in published maps and institutional affiliations.

## Authors and Affiliations

Anne Ritzer<sup>1</sup> · Tobias Roeschl<sup>1</sup>  · Sandra Nay<sup>1</sup> · Elena Rudakova<sup>1</sup> · Tilmann Volk<sup>1,2</sup> 

✉ Tilmann Volk  
tilmann.volk@fau.de

<sup>2</sup> Muscle Research Center Erlangen (MURCE), Friedrich-Alexander-Universität Erlangen-Nürnberg, 91054 Erlangen, Germany

<sup>1</sup> Institut für Zelluläre und Molekulare Physiologie, Friedrich-Alexander-Universität Erlangen-Nürnberg, Waldstraße 6, 91054 Erlangen, Germany